

THE PENNSYLVANIA STATE UNIVERSITY
SCHREYER HONORS COLLEGE

DEPARTMENT OF MECHANICAL ENGINEERING

BUILD TIME AND COST ESTIMATION OF LASER POWDER BED FUSION PROCESSES
FOR METAL ADDITIVE MANUFACTURING

MATTHEW JOHN MIDEA III
SPRING 2020

A thesis
submitted in partial fulfillment
of the requirements
for a baccalaureate degree
in Mechanical Engineering
with honors in Mechanical Engineering

Reviewed and approved* by the following:

Timothy W. Simpson
Paul Morrow Professor in Engineering Design and Manufacturing
Thesis Supervisor

Anne Martin
Assistant Professor in Mechanical Engineering
Honors Adviser

* Electronic signatures are on file in the Schreyer Honors College.

ABSTRACT

Metal additive manufacturing has changed substantially over the past few decades with advancements and improvements to the different layer-by-layer processes available. A common issue when considering whether or not to additively manufacturing a component is that most cost models are theoretical in nature, and they assume that the build time is known. Without accurate build time information, however, cost estimates will be erroneous, and sound economic decisions cannot be made. This research develops a cost model that takes in easily available data about a part, specifically its volume and height along with material, and outputs the cost of a build on different laser powder bed fusion systems used for metal additive manufacturing. Specifically, this project examines the EOS M 280, Renishaw AM250, Renishaw AM400, and Renishaw RenAM 500Q. Build time data was collected from various sources, including a Renishaw Solutions Center that additively manufactures parts for companies, and comparisons were made between the different platforms. A build time model was designed from the data from the four PBF systems. This build time model was utilized in the creation of a new cost model that does not require build time to be known. Using these models, builds with known dimensions and materials could have their costs estimated for the EOS M 280, Renishaw AM250, Renishaw AM400, and Renishaw RenAM 500Q. Future studies could inspect the differences between this model and one with other systems from other manufacturers.

TABLE OF CONTENTS

LIST OF FIGURES	iv
LIST OF TABLES	v
ACKNOWLEDGEMENTS	vi
Chapter 1 Introduction and Background.....	1
1.1 Powder Bed Fusion	1
1.2 Powder Bed Fusion Manufacturers	4
1.3 Laser Powder Bed Fusion Machines	4
1.3.1 EOS M 280.....	5
1.3.2 Renishaw AM250, AM 400, and RenAM 500Q.....	6
1.4 Outline of the Thesis	8
Chapter 2 Background	9
2.1 Existing Cost Models	9
2.2 Other Cost Considerations	11
Chapter 3 Development of Cost Model Components	14
3.1 Cost of Electricity	14
3.2 Cost of the Materials	15
3.3 Cost of the Powder Bed Fusion System	17
3.4 Cost of Post-Processing.....	18
3.5 Build Time Estimation	19
3.6 Build Time Estimation with Real Data	21
Chapter 4 Development and Analysis of the Cost Model.....	27
4.1 Creating the Cost Model	27
4.2 Error Analysis	31
Chapter 5 Implications, Contributions, and Further Research.....	34
5.1 Implications.....	34
5.2 Contributions.....	35
5.3 Future Work	35
Appendix A Thingiverse Data	37
Appendix B EOS M 280 Data	38

Appendix C Renishaw AM250 Data	39
Appendix D Renishaw AM400 Data	42
Appendix E Renishaw RenAM 500Q Data	44
BIBLIOGRAPHY.....	45

LIST OF FIGURES

Figure 1. Diagram of laser powder bed fusion [5]	3
Figure 2. EOS M 280 [14]	5
Figure 3. Renishaw's AM250 system [15]	6
Figure 4. Renishaw's AM 400 system [16]	7
Figure 5. Renishaw's RenAM 500Q system [17]	8
Figure 6. Additively Manufactured Part Consolidation for an Aircraft Duct [22]	12
Figure 7. Before and after postprocessing of a 3D printed titanium part [35].	18
Figure 8. Comparison of time to build with number of layers using Equation 7 and the real times	23
Figure 9. Comparison of time to build with volume using Equation 7 and the real times.....	24
Figure 10. Comparison of predicted and real build times based on number of parts.....	25
Figure 11. Cost breakdown by percentage for an example part.....	29
Figure 12. Cost breakdown by total cost for an example part	30
Figure 13. Comparison of build time with height using Equation 6 and the software's predictions	32
Figure 14. Comparison of build time with volume using Equation 6 and the software's predictions	33

LIST OF TABLES

Table 1. Material Properties and Prices	16
Table 2. Values for an example build	28
Table 3. Real build time-based equations and their p-values.....	31

ACKNOWLEDGEMENTS

There were many people who assisted me throughout the work on my thesis. I would first like to thank Dr. Timothy Simpson for guiding and supervising this project. I would also like to thank Dr. Anne Martin for all her assistance as an advisor over my entire undergraduate career. I am deeply indebted to Mark Kirby and Renishaw Canada who provided me with data that was pivotal to the results of this project. I could not have completed this thesis without his help. Thank you also goes to Nathaniel Tsai, Sun Angubolkul, and Samyak Jain for working with me in the early days of this project. Your cooperation has helped me write this final thesis, and I doubt I would have arrived here without your teamwork.

I want to say thank you to the Schreyer Honors College and the Harmon family for providing me financial assistance throughout my undergraduate degree. Finally, thanks to my friends and family who have supported me through these past four years of college.

Chapter 1

Introduction and Background

Additive manufacturing (AM) has changed the landscape of mechanical design. Since its inception, AM has had a tremendous effect on industry. Between 2016 and 2017, the industry had an increase in system sales of approximately 80% [1]. Metal AM has also been growing at a very high rate in some industries. For instance, AM uses in the medical and aerospace industries are projected to grow by 26% and 23%, respectively, by 2025 with the majority a factor of metal AM [2]. With a large growth to the industry, cost models have become a necessity for determining the value of adopting metal AM.

There are a variety of models that study different aspects of costs. Models range from examining theoretical aspects of a print job while others have a specific focus on a single aspect. Current cost modeling takes time to build as a known variable. This thesis creates a cost model for several laser powder bed fusion systems with inputs of part parameters and an output of cost of a build where time to build is an unknown. Without time to build as a parameter, this model would allow for an easier adoption of metal AM by businesses.

1.1 Powder Bed Fusion

Additive manufacturing is defined by ASTM standard F2792 as, “a process of joining materials to make objects from 3D model data, usually layer upon layer, as opposed to subtractive manufacturing methodologies” [3]. Several methods exist for AM that use a variety of materials ranging from polymers to metal alloys. Powder bed fusion (PBF) is one of the major

metal 3D printing methods. Even in this category, there are more subcategories based on the different types of PBF including direct metal laser sintering (DMLS), electron beam melting (E-BEAM), and selective laser melting (SLM) [4].

While each of these variants of PBF have unique aspects, they all follow the same general process. Specifically, powder bed fusion is defined by ASTM standard F2792 as, “an additive manufacturing process in which thermal energy selectively fuses regions of a powder bed” [3]. The first step in this is to create a toolpath from a computer-aided design (CAD) file for the desired part and transfer it to the machine. Once the machine is calibrated, powder is placed in the machine prior to the build. Powder is spread across the build platform, and the laser (or electron beam) is directed to locations where the material should be melted according to the toolpath. Once a layer is done, the platform is lowered by a certain height, a roller or spreader recoats the build platform with powder, and the new powder is melted to create the next layer. This process repeats until the part is finished. A visual representation of the laser PBF process can be seen in Figure 1.

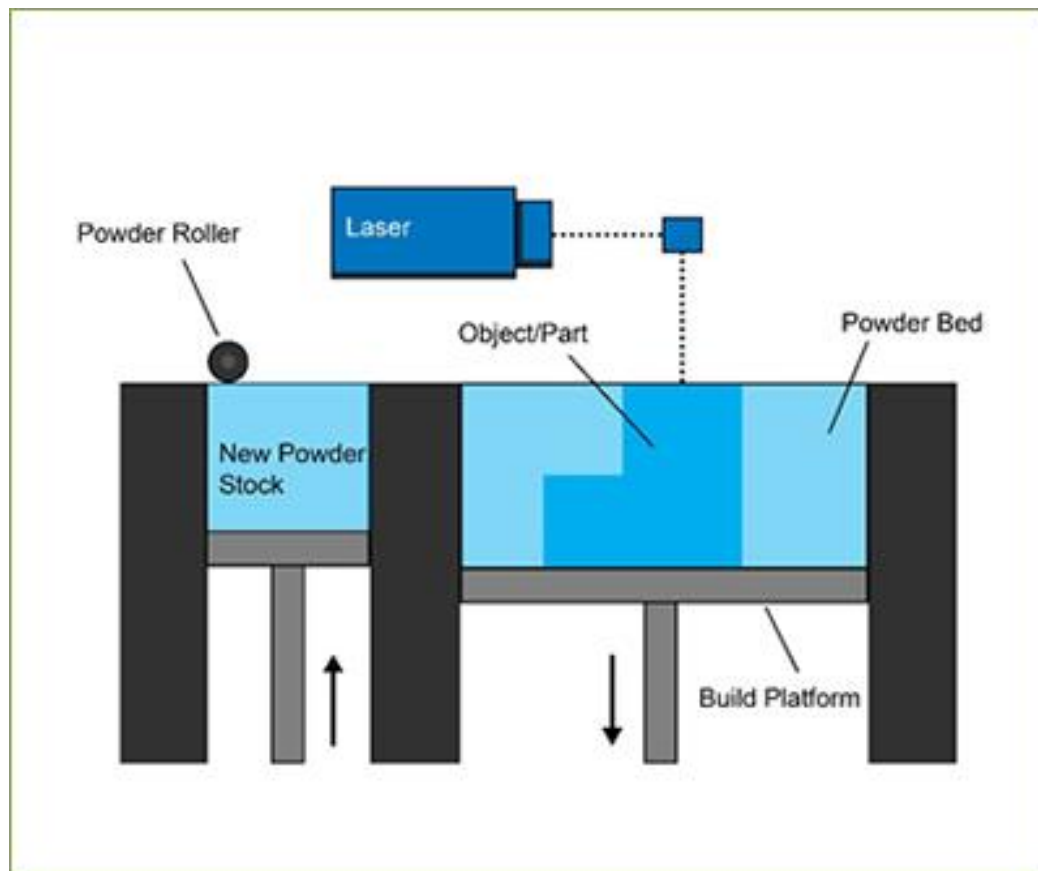


Figure 1. Diagram of laser powder bed fusion [5]

Powder bed fusion has a substantial amount of potential, given its precision and ability to add complexity without adding cost. However, it is a very time-consuming process, the material is more expensive in its powder form, and the upfront capital investment for machines is high. As the industry grows, there will be more of a demand of the material. This increase in demand will eventually lead to a decrease in material cost, which will drive further adoption. Moreover, improved technology will lead to faster build rates; so, overall the process of PBF should become substantially more viable over time.

1.2 Powder Bed Fusion Manufacturers

There are a variety of PBF printer manufacturers in this growing market. However, several have separated themselves from the rest of the pack through their prevalence and innovations. Some of the largest and most established companies include EOS [6], Renishaw [7], SLM Solutions [8], 3D Systems [9], and GE Additive [10]. EOS is a German company known for supplying industrial-grade direct metal laser sintering (DMLS) printers. They are currently the market leader in terms of sales and installations of laser PBF systems [11]. Additionally, the printers include EOSTATE, a software for monitoring various parameters during a print [12]. Renishaw, based in the United Kingdom, is another signature manufacturer of laser PBF systems. SLM Solutions, headquartered in Germany, derives its name from their process of selective laser melting (SLM) which is similar to DMLS. 3D Systems is an American company that focuses on a different offshoot of DMLS: Direct Metal Printing (DMP). They acquired their laser PBF technology by purchasing the French-based company, Phenix Systems, and then the Belgium-based company LayerWise. According to 3D Systems, DMP results in better surface finishing and more consistent quality [13]. GE Additive is the other major player in the market. They acquired the companies Concept Laser and Arcam in 2016 and 2017 respectively. Both of these companies were major forces in the market at the time.

1.3 Laser Powder Bed Fusion Machines

For the purpose of this thesis, the focus is going to be on EOS and Renishaw laser PBF machines due to availability of data.

1.3.1 EOS M 280

EOS produces a variety of laser PBF systems. Their M 280 and M 290 printers are often used as a standard in the additive metal industry. The Center for Innovative Materials Processing through Direct Digital Deposition (CIMP-3D) in State College uses an M 280, and as such, that printer will be used for one of the cost models developed in this work. The M 280 is a DMLS system that uses a 200 or 400 Watt ytterbium fiber laser to melt the metal powder. This machine has a build volume of 250 by 250 by 325 mm. The scan speed reaches up to 70 mm/s. An image of the M 280 can be seen in Figure 2.



Figure 2. EOS M 280 [14]

The M 280 system can use a variety of metal powders including steel, aluminum, nickel-based super-alloys, cobalt chrome, and titanium. It also uses either argon or nitrogen gas in the build chamber depending on the powder used.

1.3.2 Renishaw AM250, AM 400, and RenAM 500Q

Renishaw, like EOS, provides a variety of laser-based powder bed fusion printers. Renishaw Canada supplied build data for this project; so, data from several Renishaw printers is used. First, the AM250 has a build volume of 250 by 250 by 300 mm and a 200 W laser. For the purpose of this project, all data collected for the AM250 is using 316L stainless steel as the material. The AM250 system can be seen in Figure 3.



Figure 3. Renishaw's AM250 system [15]

The AM 400 is an updated version of the AM250, and as such, it can perform all of the same tasks. Thus, it has similar specifications as the AM250 with a few additional features, namely, a 400 W laser instead of a 200 W laser. The data from this printer used a titanium alloy

(Ti-6Al-4V) as the material. The AM 400 is shown in Figure 4 and looks nearly identical to the AM250 if it were not for the text on the top left of the system.



Figure 4. Renishaw's AM 400 system [16]

Finally, the RenAM 500Q is the last printer this thesis studies. It has a build volume of 250 by 250 by 350 mm. Instead of only having one laser, the RenAM 500Q has four 400 W lasers that run simultaneously. Like the AM 400, the data collected on the RenAM 500Q is for builds of Ti-6Al-4V. An image of this printer can be seen in Figure 5.

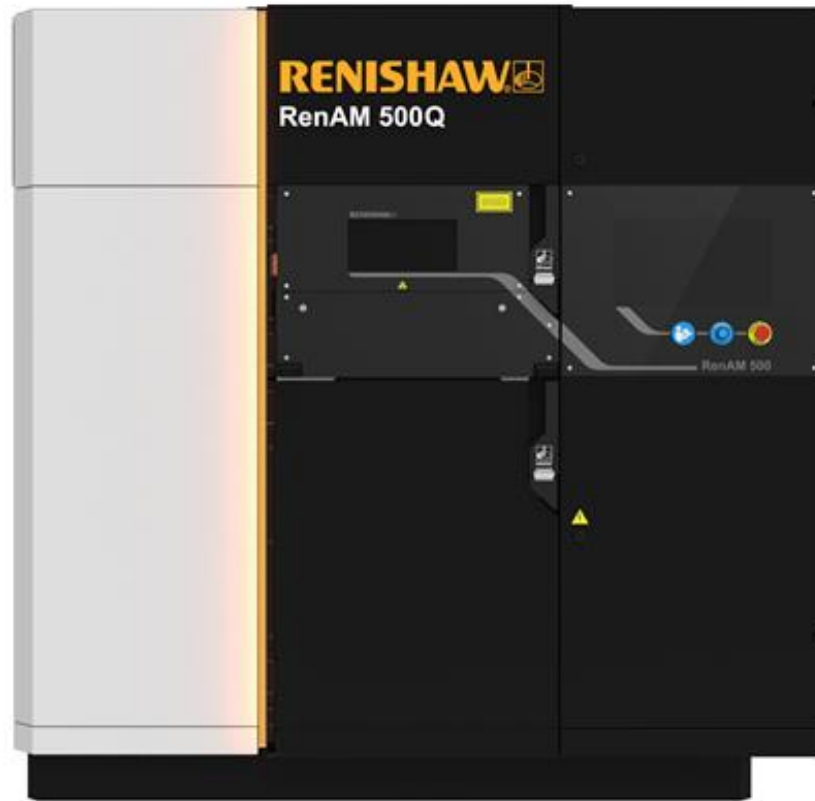


Figure 5. Renishaw's RenAM 500Q system [17]

1.4 Outline of the Thesis

This thesis investigates the current state of built time estimates and cost models for laser PBF systems and develops a cost model based on empirical data. Chapter 1 covered background information on laser-based powder bed fusion and specific commercial systems from EOS and Renishaw. Chapter 2 reviews existing cost models in the literature as well as other considerations that are not explicitly detailed in many cost models. In Chapter 3, non-part dependent factors utilized in the cost model are discussed. The focus of Chapter 4 is the formulation of both the build time and cost model. Finally, Chapter 5 provides final remarks and outlines further research.

Chapter 2

Background

There is no existing cost model that determines build time for the user for metal laser powder bed fusion. However, there has been some research into a general modeling of costs for a process and ways additive manufacturing have saved firms money. Chapter 2 discusses previous cost model research and factors that are not quantifiable before a part is built and tested.

2.1 Existing Cost Models

According to Yim and Rosen [18], there are four main components of overall cost: (1) printer purchase, (2) machine operation, (3) materials, and (4) labor. The printer purchase portion of the overall cost considers the percentage of the useful lifetime of the machine for printing as well as the overall price of the printer. Operation cost is related to many factors including utilities (e.g., electricity, gas) that vary substantially based on which process is used. Material costs are dependent not only on the volume of the part and the size of the build, but also the process used and the wasted material (e.g., support structures that are removed after a build). Finally, labor is a factor that considers the time before and after the print (set up, removal, and teardown), as it takes human capital to run these processes. Yim and Rosen present a technique for calculating build time based on part and printer parameters. However, their method proved to be an underestimation of the actual build time across all three printers in their study. This thesis takes a more empirical angle to estimating build time as opposed to a theoretical model for build time.

Baumers, et al. [19] conducted a study that focused on the economics of plastic laser sintering using an EOSINT P100. Their model can be seen in Equation 1 where the C's are cost rates, P's are probabilities, N is the number of layers, n is number of product geometries, and all other letters are relevant times for each of their corresponding costs.

$$\begin{aligned}
 Cost_{Unit} \approx & \frac{\dot{C}_{Indirect} T_{Build} + C_{Direct} + \sum_{i=1}^I R_i \dot{C}_{Labour}}{n(1 - p_{reject})(1 - P(N))} + \frac{\sum_{j=1}^J S_j \dot{C}_{Labour}}{n(1 - p_{reject})} \\
 & + \frac{\sum_{k=1}^K U_k \dot{C}_{Labour}}{(1 - p_{reject})}
 \end{aligned} \tag{1}$$

The main sources for costs can be summarized as the machine purchase, labor, material, and energy, though energy makes up a small fraction of the actual cost of any build. Given that several of these parameters can be minimized by having multiple parts in a single build, their study found that as the quantity of units in a build decreases, the price per geometry for the initial units increases. While their report is not on metal powder bed fusion, several factors remain relevant. In fact, this study examined Renishaw's AM250 and found that the data collection method and concepts were similar to SLM systems as well.

In a cost estimation paper by Piili et al. [20], the authors found that utilizing a full build platform rather than making only a single piece at a time can create massive savings. Fitting 40 pieces on a single build plate saved them 79.6% in total costs compared to printing only a single piece, and the savings only increased as more parts were added to the build plate. Machine costs made up over 90% of all costs compared to material costs and energy costs for all parts printed. Because their cost model has time to build as one of the input variables, the calculation of costs

in this paper is only possible after the build is complete. The model proposed in this thesis differs in that the theoretical cost of a part would be able to be calculated before the part is printed.

2.2 Other Cost Considerations

The possible costs avoided by switching from conventional to additive manufacturing are substantial in many cases and need to be noted, even if they are not explicitly factored into the model. Thomas and Gilbert [14] wrote that there are seven main wastes that can be avoided when using AM: (1) overproduction, (2) transportation, (3) reworks or defects, (4) over-processing, (5) motion, (6) inventory, and (7) waiting. Avoiding these wastes leads to better lean manufacturing. This is something that must be considered when choosing the manufacturing method because an additively manufactured part might be preferable when considering all of these costs despite the actual part being more expensive than a conventionally manufactured one.

One of the most important advantages to AM is part consolidation. The additional complexity that AM allows for can lead a substantially simpler part, integrating all the various functions needed in one part [21]. This process can be shown in Figure 6.

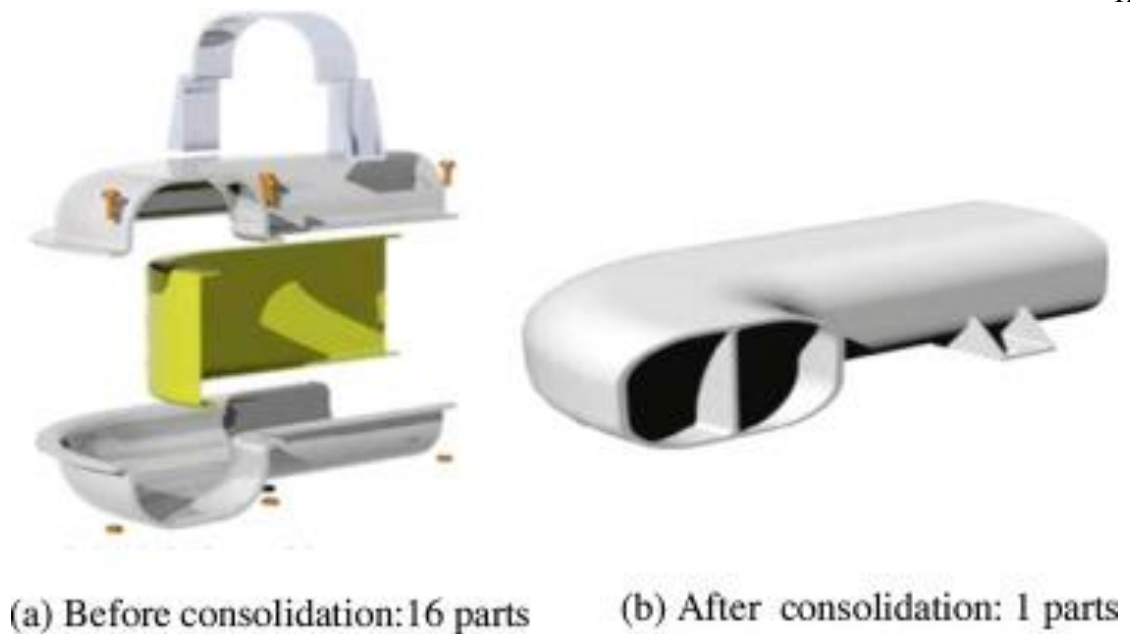


Figure 6. Additively Manufactured Part Consolidation for an Aircraft Duct [22]

Part consolidation leads to a variety of advantages including weight reduction and increased speed of production. The increased speed stems from there being fewer parts needing to be “designed, certified, inspected and manufactured” according to 3DEO [23]. This benefit occurs on a case-by-case basis, and it would be nearly impossible to factor this into a single cost model. Despite that, these design techniques and hidden cost savings are important to consider, as price alone does not tell the complete story.

In a study by Laureijs et al. [24], engine bracket designs and associated savings were examined using a DMLS printer. For aircraft, it is very important to limit and reduce weight. It costs a significant amount of money in fuel to fly with a larger load onboard. Additive design was found to reduce weight in the bracket by 80%. While this decrease in weight of a bracket would not initially appear to substantially decrease cost, it was approximated that an AM bracket would save \$1300 to \$3000 over 10 years compared to a traditionally forged bracket. While a

manufacturer of the part might not be concerned about weight saved, it can substantially make a large cost difference further down the chain.

In closing, this chapter summarized previous cost model research for powder bed fusion and how the proposed model is different. Chapter 2 also outlined methods that AM can be used to decrease costs including reducing wastes, consolidating parts, and decreasing part weight. However, these costs will not be factored into the model because they are entirely part-dependent. Instead, the model is generalizable to any part that can be printed. The next chapter introduces the parameters of the cost model and their derivations.

Chapter 3

Development of Cost Model Components

As discussed in the previous chapter, there are many factors that drive the cost of a metal AM part made by laser powder bed fusion (PBF). They can range from powder and electricity to heat treating and post-processing a component. Each factor has several aspects that vary from machine to machine and build to build. This chapter establishes the foundation for the proposed cost model by discussing in detail the specific factors that are used in the cost model as well as their explanations. Chapter 3 discusses the components of the cost model related to electricity, the materials, the PBF system, post-processing, and time to build. Chapter 4 integrates them into an overall cost model that is used for analysis.

3.1 Cost of Electricity

The cost of electricity is one of the simplest portions of the cost model. In essence, there are 3 factors: (1) how long the machine is running, (2) what is the energy consumption of the machine, and (3) what is the price per kilowatt hour. According to the Energy Information Agency (EPA), the average price of electricity in the United States is 10.27 cents per kilowatt hour [25]. As for the rate of energy consumption, the amount varies from machine to machine. According to EOS, the maximum power level of the M 280 is 8.5 kW during a build [26]. This is the worst-case scenario for this printer, and even then, the price per hour of operation is 87.3 cents per hour. For the most part, the system operates well below this number at an average of 3.2 kW for a price of 32.9 cents per hour [26]. As for the AM250, Faludi et al. [27] found that

the printer consumes approximately 1 kW on average for a relatively normal build. The AM400 was found to use around 1.6 kW during a build [28]. These correspond to costs of 10.3 and 16.4 cents per hour for the AM250 and AM400, respectively.

There is less available data on the RenAM 500Q. Given that it has four 500W lasers, it should have a minimum power level of 2 kW while all four lasers are operating, likely higher than the EOS machine. Overall, the cost of electricity is one of the smallest factors in the cost model, and as such, is not be a heavy emphasis in the model.

3.2 Cost of the Materials

The calculation of the cost of materials is not as simple as multiplying the volume of the part by the price of that volume of material as other materials are used during the build. There are two main materials used in a build: (1) metal powder and (2) inert gases.

Metal powder is the first of the material costs. Powder prices vary across sellers. For example, from EOS, the cost of aluminum (ALSi10Mg) is around \$152 per kg [29]. On the other hand, through a quote from Carpenter Additive, aluminum is approximately \$87.5 per kg (Imperial, PA). This difference can be due to several factors including time of the quote as well as the amount and size of powder being purchased. Powder ranges in the tens of microns in diameter, often between 10 and 70. If the powder is too large, it can cause poor flow and unpredictable layers. Several materials and prices are shown on Table 1 with the densities from EOS and derived price per cubic meter [30].

Table 1. Material Properties and Prices

	Density (g/cm ³)	Price from Carpenter Additive (\$/kg)	Price from Carpenter Additive (\$/cm ³)	Price from EOS (\$/kg)	Price from EOS (\$/cm ³)
Aluminum (AlSi10Mg)	2.7	87.5	0.24	152	0.41
Titanium (Ti-6Al-4V)	4.4	275	1.21	617	2.71
Stainless Steel (17-4)	7.7	70	0.54	105	0.81
Nickel (Inconel 718)	8.2	N/A	N/A	192	1.57
Cobalt Chrome (CoCrMo)	8.3	N/A	N/A	330	2.74

The second part of materials is the gas consumed during the printing process. There are two main gases used for the printing process: (1) argon and (2) nitrogen. The one used can vary by machine and by material. Renishaw makes it a point to use argon for all relevant machines and materials due to it being more economical [31]. On the other hand, EOS varies the gas based on material. For example, the M 280 uses nitrogen for stainless steel and cobalt chrome and argon for titanium, nickel, and aluminum.

The argon gas consumption during a build is less than 30, 50, and 50 L/hr for the AM250, AM400, and RenAM 500Q, respectively. Also, the initial filling of the chamber of argon is approximately 600 L for the AM250 and AM400 and 1200 L for the RenAM 500Q. According to Weilhammer, the average gas consumption during a job is about 5-10 L/min for the EOS M 280 [32].

As for the price of these gases, it too varies over time, type, and provider. From Airgas, the price of nitrogen is approximately \$0.07 per cubic foot, and the price of argon is approximately \$0.29 per cubic foot [33]. Once the build time is known, it is possible to calculate the cost of the gas consumed in a build.

3.3 Cost of the Powder Bed Fusion System

Metal AM systems range in price, reaching as high as a few million dollars. Given that these printers will not work forever and will become outdated, the time it takes to complete a build must be included in the model. To calculate this expense, the lifetime of the printer, print time, setup time, and price of the printer must be known. The cost of the printer for a single build, $C_{printer}$, can be calculated using Equation 2:

$$C_{printer} = P_{initial} \frac{T_{build} + T_{setup}}{T_{life}} \quad (2)$$

where $P_{initial}$ is the initial cost of the printer in dollars, T_{build} is the estimated time to build in hours, and T_{setup} is the setup time for the build in hours. For the lifetime of the printer, this model will use a lifespan of 8 years for 5000 hours per year (or 40000 hours total), similar to the values Baumer, et al. use in their study [19]. The time of the build is part dependent and is estimated for the four printers in this study in Chapter 4.

The setup time includes inputting parameters, preparing materials safely, and fixing the platform for the run. Setup time is operator dependent, and for this model, a value of 2 hours is used, like what Barclift et al. [34] did when studying depreciation reused powder feedstocks. Finally, the initial cost of the printer varies by manufacturer and time of the quote. Thus, the values in this thesis serve as a guideline rather than a definitive quote. EOS quoted the M 280 for approximately \$900,000 (Novi, MI). Renishaw quoted the AM250 and AM400 for approximately \$675,000 and the RenAM 500Q for \$850,000 (West Dundee, IL). These values

are relevant at the time of writing this and the price may fluctuate. For the purpose of this thesis, these are the values used.

3.4 Cost of Post-Processing

After PBF, AM parts can be rough and unfinished. If used in this state, they may not meet the requirements needed for the final part. Figure 7 shows how dramatic this difference between a raw and post-processed part can be.



Figure 7. Before and after postprocessing of a 3D printed titanium part [35].

There are many post-processing methods that are available for metal AM parts. The first step is stress relief. This is necessary because there are internal stresses in a part as it builds layer after layer. If not done properly, removal of the part from the plate can cause warping or cracks. Wire EDM (electrical discharge machine) is the next step. This process is done to remove the

printed part from the build plate. After removing the part from the plate, a part needs to be heat treated to improve the mechanical properties of the part. Machining and surface treatments are the final steps. These two processes are done to ensure that the part meets the design requirements in terms of dimensions and to improve the surface roughness and quality.

Estimates for outsourcing these processes do vary, but according to Solar Atmospheres (Hermitage, PA), a heat-treating company, stress relief can fluctuate around \$450-\$600. Wire EDM costs range from \$15 a part to \$450 a plate. According to Simpson, heat treatment can range from \$500-\$2000, and machining and surface treatments can range dramatically for a part [36]. Because these prices vary over time and from company to company, they are calculated last in the model and as a secondary number for the overall cost of the total build. Additionally, the cost of machining and surface treatment is not included as this number ranges significantly based on the specifics of each build.

3.5 Build Time Estimation

Build time is an integral factor for determine the costs of electricity and running the PBF system. There are three main steps taken to develop the model: (1) determine relevant factors for the build time estimate, (2) examine software predictions, and (3) use print data to create a finalized model.

The first step for estimating build time is to examine part parameters that may be relevant. Rickenbacher, et al. [37] proposed a build time model for SLM processes that can be seen in Equation 3:

$$T_{build} = \frac{a_0}{\sum_i N_i} + T_L(P_i) + a_2 * V(P_i) + a_3 * S_{Supp}(P_i) + a_4 + a_5 * S(P_i) \quad (3)$$

where T_{build} is the building time in hours, a 's are regression coefficients, N_i is the quantity of parts with i th geometry, T_L is a layer-dependent fraction in hours, P_i is part i , V is the volume in mm^3 , S_{Supp} is the surface area of support structures in mm^2 , and S is the surface area of the part in mm^2 . Several factors including the correlation coefficients, layer-dependent fraction, and surface areas are not immediately apparent or easily estimated when designing a part. Key takeaways from their equation is that volume, number of parts, and height play important roles in build time estimation.

The next step is to examine the theoretical estimations of the build time. The purpose of this step is to determine if the relevant parameters previously found align with software predictions. A high correlation between the parameters and build time of the software would suggest that the parameters chosen are relevant. It is also to show that the model using real data differs from that of a theoretical model.

The software used to gather this theoretical data was Netfabb, Autodesk's toolset for AM [38], and 27 parts were collected from Thingiverse and spanned a variety of heights (4-257 mm) and volumes (0.097-437.22 cm^3). More information on these parts is available in Appendix A. The EOS M 280 is the only system in this study for which build time estimates are available on Netfabb. Using a multiple variable regression analysis, a combination of several factors is examined. Specifically, build height H (mm) and part volume V (cm^3) are regressed against the Netfabb's time to build $T_{build,Net}$ (hrs) to form Equation 4:

$$T_{build,net} = 0.0361 + 0.0554 * H + 0.200 * V \quad (4)$$

The R-squared value is found to be 0.999, a value indicating that this Equation 4's prediction has a high correlation with the values predicted by Netfabb.

There is a strong relationship between build height, part volume, and build time based on Netfabb. The number of parts, N , is added next to the regression model. Several of the same part were added to the build plate to examine the impact on build time. The volume of these additional parts is included in V_{total} in Equation 5:

$$T_{build} = 0.0450 + 0.0554 * H + 0.200 * V_{total} - 0.0112 * N \quad (5)$$

The coefficients for height and volume are nearly unchanged from Equation 4. The coefficient for N is very low, indicating that the number of parts contributes very little to time to build, outside the additional volume added. The p-value of this coefficient is 0.49, showing that the exact value is not significant. The coefficients for H and V_{total} have p-values of 2.3E-40 and 8.8E-65, so they are significant.

3.6 Build Time Estimation with Real Data

Using real data collected from 4 builds on the EOS M 280, a new equation is formulated. This real data can be found in Appendix B. Because the 4 builds each only have one part per build, the number of parts N is not a factor for Equation 6:

$$T_{build} = 4.83 + 0.0330 * V + 0.0801 * H \quad (6)$$

Equation 6 has a R-squared value of 0.999. The three p-values of these coefficients are 0.61, 0.06, and 0.27 from left to right, respectively, meaning that no coefficients are significant.

The AM250 is the next system examined. The data from Renishaw included time, part volume, support material volume, number of layers, and number of parts. Layers do not give an exact value of the height of a build, but it still gives an indication of the impact height. The AM250 as well as the AM400 and RenAM 500Q have a viable layer thickness of 20 to 100 μ m, and these data points fall into that range. More specifically, Renishaw noted that for their layer thickness for the AM250 data is nearly all 40 microns, the AM400 is mainly 30 microns, and the RenAM 500Q is split between 30 and 60 microns. The 85 data points for the AM250 can be found in Appendix C. With only accounting for the number of layers and volume of the part, an R-squared of 0.87 is calculated for Equation 7:

$$T_{build} = -1.60 + 0.154 * V + 0.00414 * L \quad (7)$$

where L is the number of layers. The p-values for the coefficients of V and L are 5.5E-29 and 1.4E-5, and because they are less than 0.05, they are significant. This is shown in Figures 8 and 9 where the predicted estimate is the output of Equation 7 for each of the parts and the real data is the result of the Renishaw print.

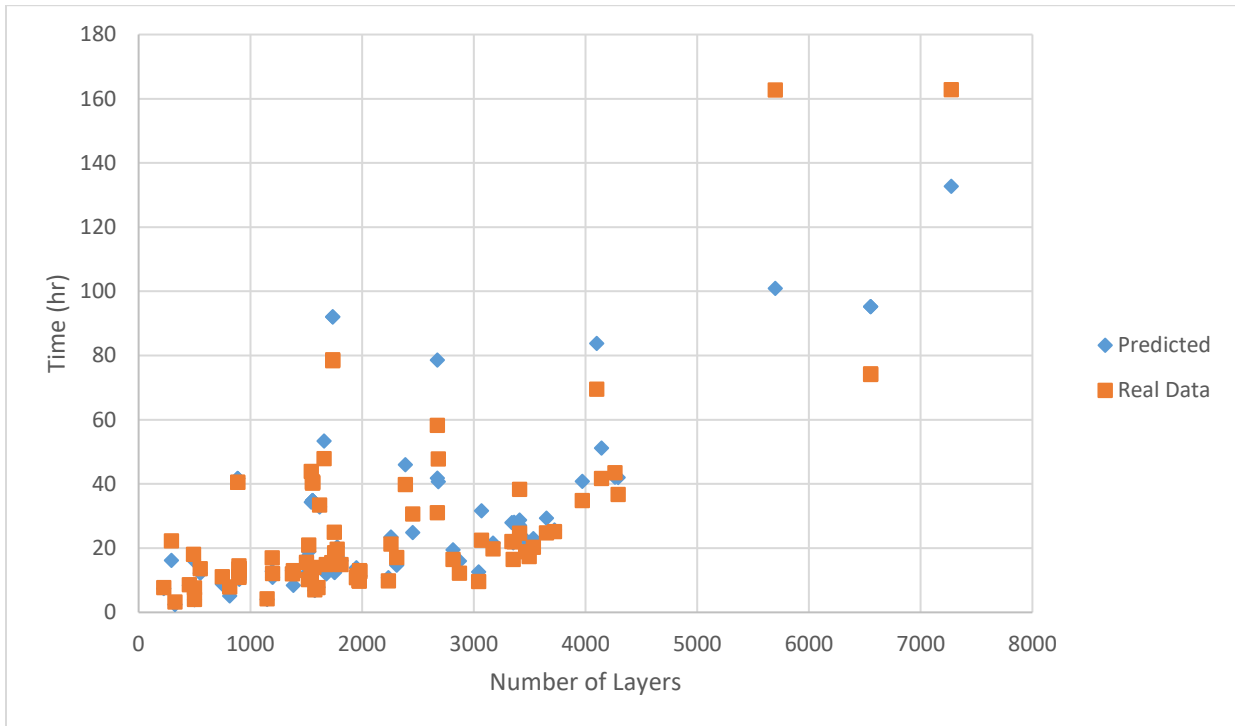


Figure 8. Comparison of time to build with number of layers using Equation 7 and the real times

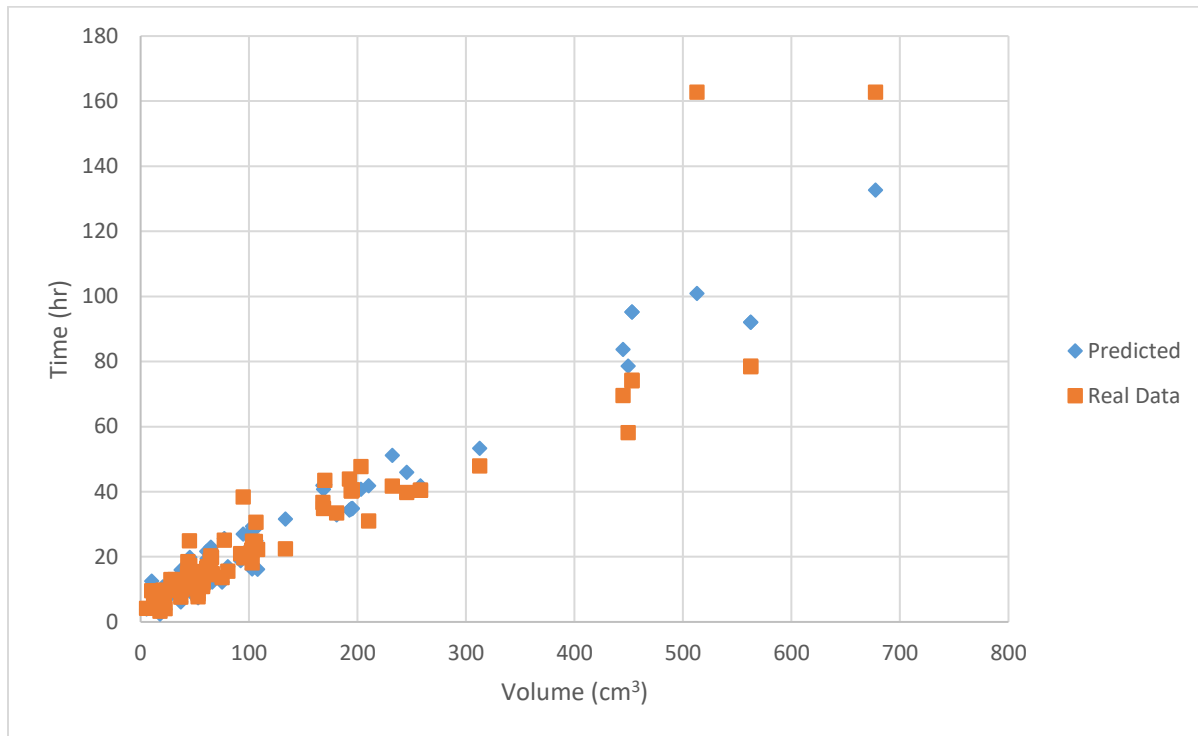


Figure 9. Comparison of time to build with volume using Equation 7 and the real times

While not perfect, the general trend shows that the predicted build times line up relatively well with the real data, although the equation is less reliable for longer builds. The number of parts makes very little difference. Using only the number of parts as a parameter, Figure 10 can be made. Exclusively considering the number of parts, the R-squared is 0.0026, indicating little to no impact on time to build.

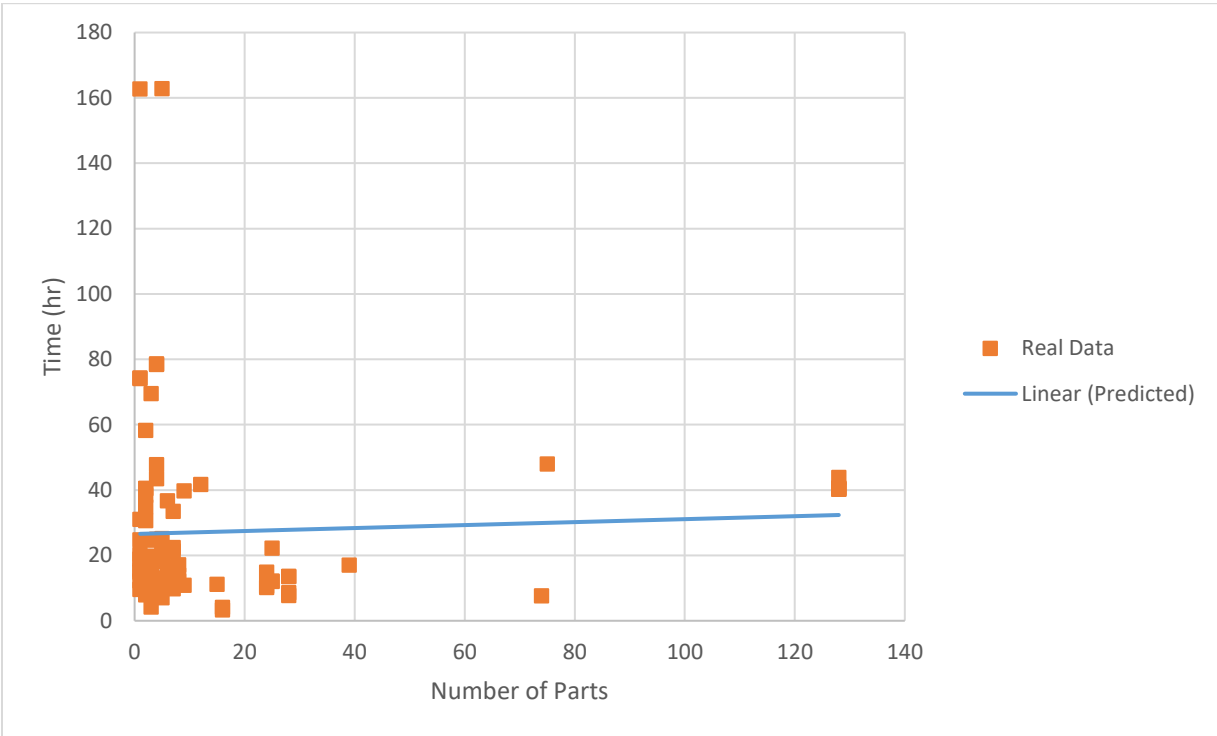


Figure 10. Comparison of predicted and real build times based on number of parts

The 61 data points for the AM400 are presented in Appendix D. Equation 8 is a regression using only the volume of the part and the number of layers:

$$T_{build} = 1.05 + 0.0488 * V + 0.00439 * L \quad (8)$$

with the corresponding R-squared value of 0.73.

Renishaw's RenAM 500Q is the final printer inspected using 22 data points as shown in Appendix E. Using part volume and number of layers, Equation 9 is derived:

$$T_{build} = -0.648 + 0.00766 * V + 0.00602 * L \quad (9)$$

where there is an R-squared value of 0.86.

Chapter 3 discussed relevant parameters used in the cost modeling process. Specifically, it covered electricity, powder metal, inert gas, PBF system, post-processing, and build time.

Chapter 4 develops the cost model and analyzes information from both the build time and cost models.

Chapter 4

Development and Analysis of the Cost Model

Chapter 4 presents the overall cost model by combining the various factors from Chapter 3. Also, Chapter 4 analyzes several of the values and discusses their reliability.

4.1 Creating the Cost Model

With the build time estimated, an equation can be made for the cost of the build. The general equation is shown in Equation 10:

$$C_{Total} = C_{printer} + C_{material} + C_{post} + C_{electricity} \quad (10)$$

where C_{Total} is the total cost of a build, $C_{printer}$ is the cost of the printer for the amount of time taken up by the build, $C_{material}$ is the cost of the materials used in the build, C_{post} is the cost of post processing, and $C_{electricity}$ is the cost of electricity. With each of these costs expanded, the new equation for total cost is shown in Equation 11:

$$C_{Total} = (P_{initial} \frac{T_{build} + T_{setup}}{T_{life}}) + (P_{elec} * T_{build} * R_{elec} + V_{build} * P_{powder} + P_{gas} * T_{build} * R_{gas}) + C_{post} \quad (11)$$

where $P_{initial}$ is the initial price of the printer in dollars, T_{build} is time to build in hours, T_{setup} is setup time in hours, T_{life} is the lifetime of the printer in hours, P_{elec} is the price of electricity in

dollars per kilowatt hour, R_{elec} is the rate electricity consumption of the machine in kilowatts, V_{build} is the volume of the build in cubic centimeters, P_{powder} is the price of the powder in dollars per cubic centimeter, P_{gas} is the price of the gas supplied in dollars per liter, and R_{gas} is the rate of gas consumption by the printer in liters per hour. All of these values can be calculated from the equations presented in Chapter 3. With the material, volume, and height of a desired build, a price can be determined for each of the four printers examined in this thesis.

To demonstrate the use of the cost model, consider a part with the following parameters: height of 50 mm, volume of 120 cm³, and material of Ti-6Al-4V. Table 2 contains the values used in this example.

Table 2. Values for an example build

	Platform			
	EOS M 280	Renishaw AM250	Renishaw AM400	Renishaw RenAM 500Q
$P_{initial}$ (\$)	900,000	675,000	675,000	850,000
T_{setup} (hr)	2	2	2	2
T_{life} (hr)	40000	40000	40000	40000
P_{elec} (\$/kWhr)	0.1027	0.1027	0.1027	0.1027
R_{elec} (kW)	3.2	1	1.6	2
V_{build} (cm ³)	120	120	120	120
P_{powder} (\$/cm ³)	1.21	1.21	1.21	1.21
P_{gas} (\$/L)	0.01024	0.01024	0.01024	0.01024
R_{gas} (L/hr)	300	30	50	50
T_{build} (hr)	12.79	22.04	14.22	10.31
$C_{printer}$	332.78	405.68	273.71	261.59
$C_{material}$	184.49	151.97	152.48	150.48
C_{post}	2000	2000	2000	2000
$C_{electricity}$	4.20	2.26	2.34	2.11
C_{Total}	2521.47	2559.91	2428.53	2414.18
C_{Total} before C_{post}	521.47	559.91	428.53	414.18

These values come with a few assumptions. The first is that the powder material is purchased through Carpenter Additive, which dictates the cost of the material. Additionally,

layer thicknesses of 40, 30, and 60 microns are used for the AM250, AM400, and RenAM 500Q respectively. With these thicknesses, the number of layers is 1250, 1667, and 833 for the AM250, AM400, and RenAM 500Q, respectively, for the example part.

The cost breakdown is graphed in Figures 11 and 12. Figure 11 plots the percentage of the total cost that each major component makes up. Figure 12 displays the total cost of the build broken down by component.

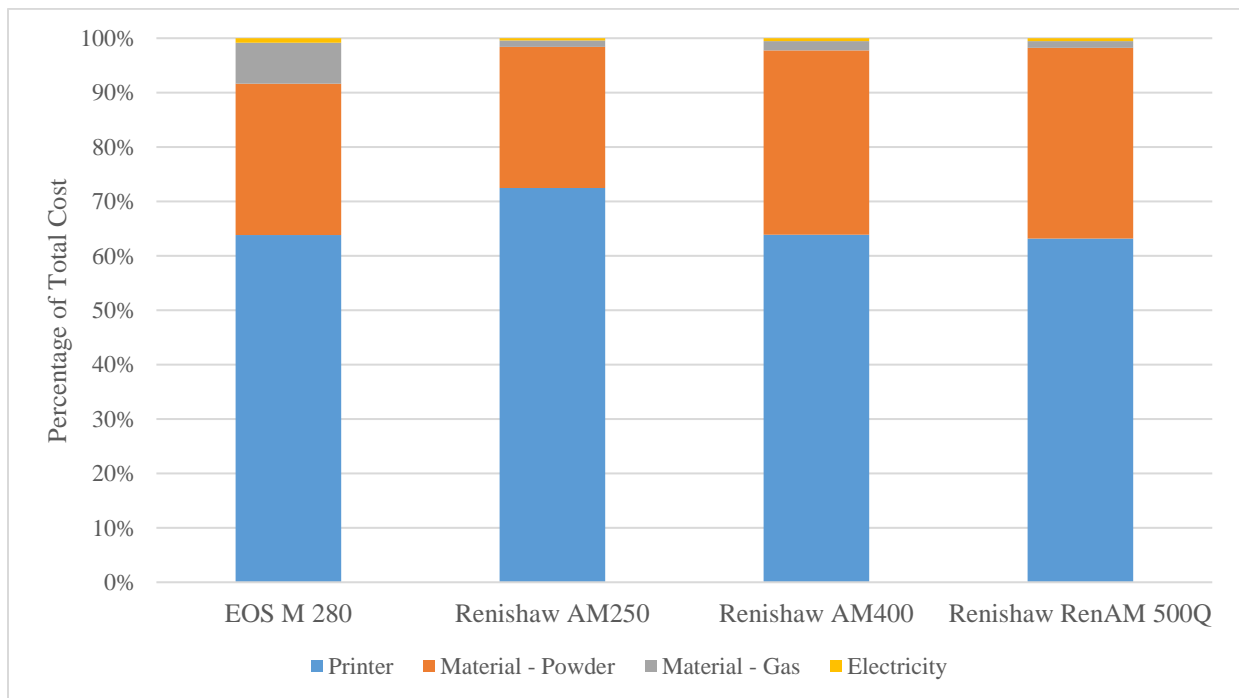


Figure 11. Cost breakdown by percentage for an example part

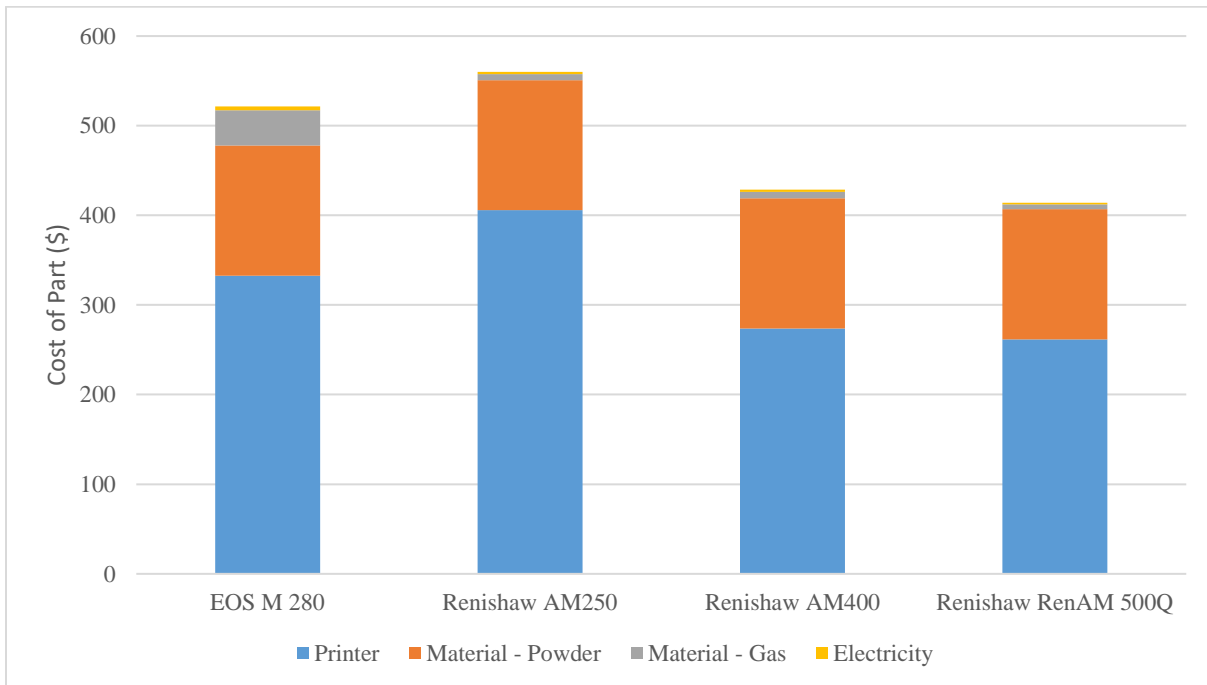


Figure 12. Cost breakdown by total cost for an example part

Overall, this example part indicates that though the EOS M 280 and the RenAM 500Q are both more expensive than the AM250, they can still be more economical for a build due to their faster print times. For this part, based on the cost and build time models, the most economical printer would be the RenAM 500Q because of its fast printing speed.

Additionally, these results indicate the most impactful components on the total cost. Electricity is such a small component, which makes practically no difference on total cost. In fact, it makes up less than 1% of total cost for each of the systems. Over 90% of total costs come from printer and powder metal costs.

4.2 Error Analysis

Because many of the costs in the model are not quantified during a build, a detailed error analysis would be difficult to perform. Rather, an analysis can be done on the specific build time estimations. For reference, Table 3 includes the relevant equations and corresponding p-values of all their coefficients.

Table 3. Real build time-based equations and their p-values

Platform	Equation	Constant	Volume Coefficient	Height or Layer Coefficient	R-Squared	Sample Size
M 280	6	4.83	0.0330	0.0800	0.999	4
	6 (p-values)	0.61	0.063	0.27	N/A	N/A
AM250	7	-1.60	0.154	0.00414	0.87	85
	7 (p-values)	0.42	5.5E-29	1.4E-5	N/A	N/A
AM400	8	1.05	0.0488	0.00439	0.72	61
	8 (p-values)	0.47	1.4E-10	1.3E-10	N/A	N/A
RenAM 500Q	9	-0.648	0.00766	0.00602	0.86	22
	9 (p-values)	0.76	0.48	5.2E-7	N/A	N/A

The highlighted cells are the ones with a p-value less than 0.05, indicating that they are statistically significant. The M 280 does not have a significant coefficient likely due to the small sample size used in this study. Therefore, a test of the equation is necessary to determine if it is relatively accurate. For this, the 27 parts from Thingiverse (in Appendix A) are plotted with Equation 6 as the time to build model prediction and Equation 4 as the software prediction as shown in Figures 13 and 14.

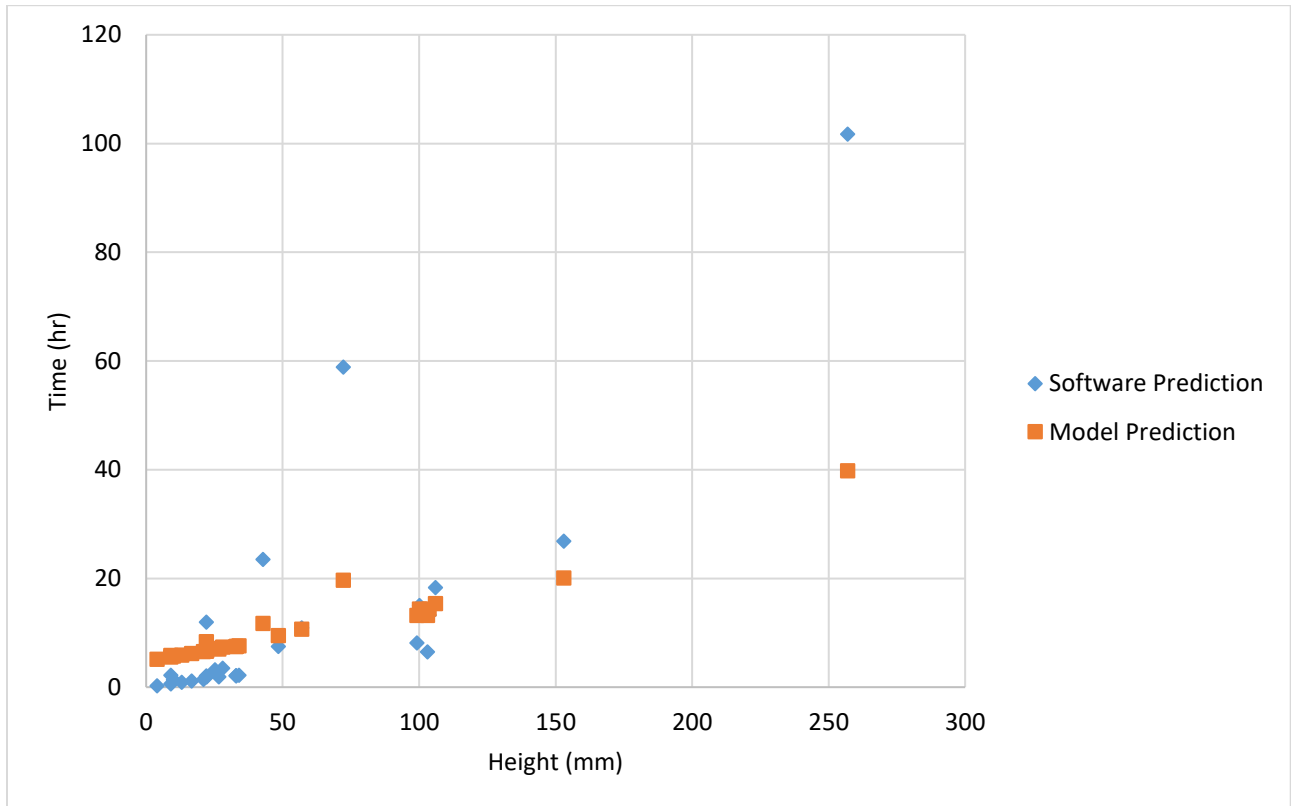


Figure 13. Comparison of build time with height using Equation 6 and the software's predictions

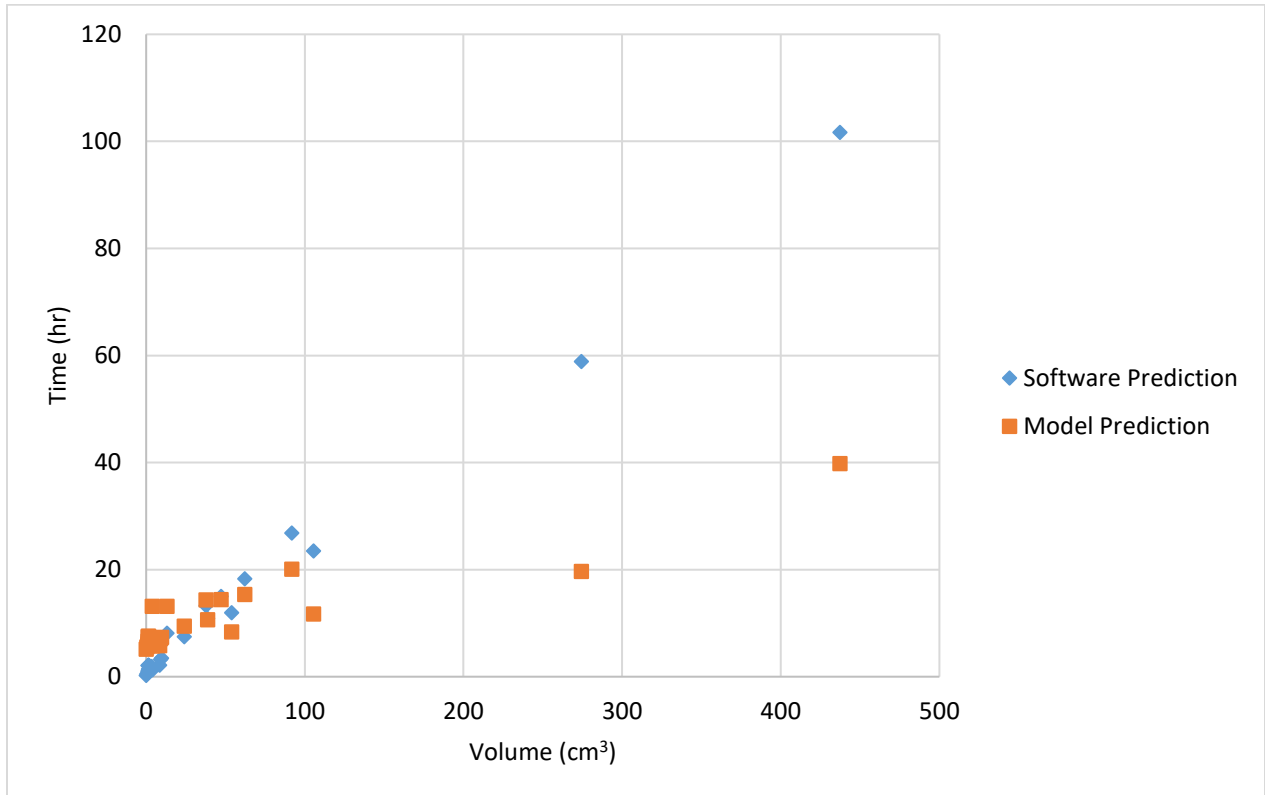


Figure 14. Comparison of build time with volume using Equation 6 and the software's predictions

Overall, this real data prediction is substantially different from the Netfabb prediction, especially at longer build times. Therefore, the model for the M 280 needs more data to determine reliable time to build model.

Finally, none of the constants in any of the equations are statistically significant. They are a correction factor to allow all data to be contained by the graph. However, even if they are not statistically significant, other portions could be. The volume and layer trends can still indicate the general cost of a build even if the constant is not significant. The implications of this along with possible future work are discussed in the next chapter.

Chapter 5

Implications, Contributions, and Further Research

This chapter examines the results of the cost model to determine the implications of the work. Also, this chapter discusses contributions from the work and possible areas for future work on this topic.

5.1 Implications

Due to the build time being substantially lower for the RenAM 500Q, determining which printer to choose for the most cost-effective part is not as simple as choosing the least expensive PBF system. With the example build from Table 2 in Chapter 4.1, the least expensive method would be to use the RenAM 500 Q, as it took 2.5 hours less than the next closest printer. However, this is only for a moderately large-sized build with a volume of 120 cubic centimeters and a height of 50 mm. For smaller builds, where the time difference is smaller, the AM400 might become more cost effective.

The build time results in Table 3 show a trend of improvement with newer systems and increased laser power. The AM 400 has a three-fold decrease in print time of volume as compared to the AM 250 while the height print time remained nearly the same. This can be accounted for with the increase of laser power from 200 to 400W as well as other improvements made over the upgrade in systems. A similar increase in print speed can be seen in the improvement in build time from the AM400 to the 500Q. With the four 400W lasers, the RenAM 500Q has a 6-fold decrease in print time of volume as compared to the AM250. Overall, this

indicates that an increase in lasers (and laser power) can lead to a substantially lower printing time, making a more expensive machine more cost-effective to build the part.

5.2 Contributions

This model examines four metal AM systems and the contributing factors to the cost of a build made with laser powder bed fusion. With the focus of creating a build time model, this model makes several contributions to metal additive manufacturing. The metal AM market is expanding, and new firms are considering entering. The build time and cost models provide important information as to when it is time to enter the market, requiring minimal information about the part to determine the cost. This model can also be utilized by firms to expedite the prototyping process and make informed decisions as to the value of having a metal AM part.

The predictability of a metal AM process is also improved. While this model uses data for four specific laser PBF systems, the sources of costs are likely to be similar, with printer and materials costs making up the majority. The four PBF systems in this model lay a groundwork for models for other specific printers in the future.

5.3 Future Work

Newer laser PBF systems bring improvements to build time, quality, functionality, and more. Examining newer systems would strengthen the model and keep it relevant. Additionally, expanding the model to include other systems would give a larger perspective on the market.

Overall, while this model looks at a few current systems, future systems and other current systems can be added to make the model more complete.

Appendix A

Thingiverse Data

BUILD NAME	TIME (HR)	VOLUME (CC)	HEIGHT (MM)	NUMBER OF PARTS
Piston Head	1.936944444	3.53	22.15	1
Piston Head	2.634722222	3.53	22.15	2
Piston Head	3.340833333	3.53	22.15	3
Piston Head	4.046944444	3.53	22.15	4
Piston Head	4.753333333	3.53	22.15	5
Wrench	1.355555556	4	10	1
Wrench	2.155555556	4	10	2
Wrench	2.955555556	4	10	3
Wrench	3.755555556	4	10	4
Wrench	4.555555556	4	10	5
Bitholder Handle	18.32416667	62.18	105.99	1
Arranque Volkswagen	1.155	1.14	16.7	1
Bolt 25x8	2.148611111	1.58	33	1
Bolt 25x8 Button	2.099444444	1.32	22	1
Bolt 25x8				
Coutnersunk	2.096388889	1.32	33	1
Bolt 25x8 Socket	2.184722222	1.48	34	1
Nut 6x9	0.586944444	0.43397	9	1
Nut Joiner 18x9	1.431944444	1.33	21	1
Threaded Rod 8x100	6.477777778	3.76	103	1
Washer 1x8.5	0.241666667	0.09713	4	1
Wingnut 6x9	0.921944444	0.98818	13	1
Reversible Hinge	2.2	8.5	9	1
Nut (Big)	23.49888889	105.59	42.85	1
Shelf Bracket	11.98805556	53.8	22.05	1
90 Deg. Angle Bracket	3.484444444	9.63	28	1
Table Leg Bracket	10.91277778	38.73	57	1
Parametric L Bracket	1.914722222	2.18	26.59	1
Triple Gear	7.504722222	24.06	48.4	1
Complex Cheese	58.89083333	274.37	72.26	1
Complex Vase	26.88138889	91.89	153	1
Chunks of Volume	15.01944444	47.26	100.17	1
Mayan Style	13.28777778	37.65	103.6	1
Nuron Cells	8.150277778	13.19	99.17	1
Finished Cylinder	101.7213889	437.22	257	1
Diagrid Bracelet	3.227777778	9.14	25.16	1

Appendix B**EOS M 280 Data**

BUILD NAME	TIME (HR)	PART VOLUME (CC)	HEIGHT (MM)	NUMBER OF PARTS
RS	30.38333	412.28	148.59	1
	3			
RP	24.23333	175.02	171.75	1
	3			
LS	31.86666	454.86	150.99	1
	7			
LP	24.88333	181.69	174.3	1
	3			

Appendix C

Renishaw AM250 Data

BUILD NAME	TIME (HR)	PART VOLUME (CC)	SUPPORT VOL (CC)	NUMBER OF LAYERS	NUMBER OF PARTS
RC102	10.95	57.03	15.76	898	3
RC103	9.983333	38.16	1.38	1973	6
RC105	4.1	22.61	0	499	16
RC107	58.23333	449.44	29.31	2673	2
RC110	31.05	210.29	14.64	2673	1
RC097	14.95	66.02	2.76	1813	24
RC144	41.76667	231.97	4.8	4142	12
RC147	8.616667	53.03	0	455	28
RC151	7.7	18.04	9.52	1606	4
RC152	22.48333	133.53	0	3069	7
RC154	11.31667	57.03	15.76	899	3
RC155	10.85	48.26	2.39	1949	9
RC156	3.3	17.76	0	324	16
RC157	38.38333	94.42	1.33	3411	2
RC159	24.73333	105.62	1.44	3411	3
RC164	43.5	169.76	76.05	4263	4
RC165	17.11667	44.15	32.87	2311	8
RC166	17.03333	61.5	18.79	1196	39
RC167	14.03333	55.89	9.49	1569	8
RC171	10.68333	36.07	0.39	1544	24
RC172	12.05	57.71	4.9	1376	4
RC173	21.33333	101.94	8.65	2260	7
RC182	13.05	27.95	1.64	1384	4
RC183	18.58333	43.65	1.52	1754	4
RC184	14.55	65.92	14.25	899	6
RC185	9.716667	28.91	2.56	1974	4
RC186	7.766667	53.03	0	224	28
RC187	10.23333	52.19	0	1519	24
RC197	16.55	61.16	0	2814	6
RC198	13.65	75.07	0	552	28
RC199	12.16667	49.43	10.1	1200	8
RC201	12.08333	37.58	0.41	1546	25
RC202	12.18333	37.58	0.41	1544	25
RC203	43.9	192.4	2.12	1546	128
RC204	4.233333	5.55	1.29	1149	3
RC205	21.03333	92.34	28.06	1522	6

RC207	78.45	562.37	0	1736	4
RC209	13.05	31.29	20.59	1977	4
RC210	39.8	245.17	12.08	2388	9
RC212	47.95	312.58	0	1660	75
RC217	7.683333	37.08	0	500	74
RC219	78.66667	562.37	0	1736	4
RC220	40.5	257.96	33.37	887	2
RC222	40.53333	257.96	33.37	887	2
RC226	19.73333	95.12	15.89	1776	5
RC228	22.28333	107.7	13.36	295	25
RC233	13.63333	57.42	14.25	902	3
RC234	11.5	41.12	4.35	1955	4
RC235	13.53333	53.03	0	902	28
RC237	13.48333	57.42	14.25	902	3
RC238	7.933333	22.09	17.75	814	2
RC239	25	45.01	71.85	1752	4
RC240	17.36667	45.21	11.3	3497	3
RC242	30.66667	106.25	50.68	2454	2
RC246	40.3	194.37	2.15	1556	128
RC250	16.5	61	0	3353	3
RC251	69.58333	444.66	0	4100	3
RC252	22.03333	102.48	1.43	3362	5
RC253	22.11667	102.48	1.5	3341	5
RC254	14.95	43.19	17.66	1679	1
RC256	12.7	31.06	2.39	1980	5
RC259	11.13333	47.36	10.97	750	15
RC260	9.6	10.29	3.87	3044	1
RC264	33.5	180.6	27.25	1620	7
RC266	7.033333	12.1	7.95	1578	5
RC267	9.816667	20.63	7.14	2235	7
RC268	20.31667	64.76	10.85	3533	1
RC270	18.88333	64.29	6.05	3464	1
RC271	25.18333	77.05	15	3722	5
RC272	36.73333	167.86	13.19	4292	6
RC273	19.8	65.37	18.1	3173	3
RC277	15.5	57.53	23.12	1729	6
RC279	74.16667	452.85	0	6553	1
RC280	74.35	452.85	0	6553	1
RC285	18.15	102.93	0	491	5
RC286	34.85	168.61	17.66	3972	2
RC288	15.66667	80.46	0	1503	1
RC292	162.7667	512.83	122.48	5700	1
RC295	162.8333	677.46	27.32	7273	5

RC297	24.81667	103.21	13.53	3650	1
RC299	12.25	37.42	1.86	2872	1
RC301	40.3	194.37	2.15	1556	128
RC302	40.58333	195.29	2.13	1556	128
RC305	40.63333	195.02	2.14	1556	128
RC308	47.76667	203.06	75.98	2682	4

Appendix D

Renishaw AM400 Data

BUILD NAME	TIME (HR)	PART VOLUME (CC)	SUPPORT VOLUME (CC)	NUMBER OF LAYERS	NUMBER OF PARTS
RC114	5.8333333	21.04	6.45	1413	24
RC115	4.5833333	56.33	0	354	37
RC116	4.9666667	45.39	2.21	464	38
RC117	3.2333333	39.52	0	464	16
RC118	6.2166667	74.41	0	966	13
RC121	6.0666667	77.62	5.72	572	11
RC122	13.1333333	108.43	0.1	1709	23
RC123	3.2	24.34	0	548	22
RC124	6.5833333	23.08	4.23	1003	10
RC126	6.2833333	40.78	10.38	820	11
RC127	2.8166667	15.93	3.81	547	19
RC130	32	583.92	6.7	1504	57
RC134	31.766667	583.92	6.7	1504	57
RC135	10.2	99.63	19.54	684	63
RC139	4.9833333	77.9	0	354	44
RC140	33.3	614	6.63	1518	48
RC143	16.816667	145.43	70.67	2345	4
RC145	3.8833333	63.34	0	354	24
RC146	2.3666667	31.67	0	355	12
RC149	6.3666667	63.17	8.37	1045	18
RC150	1.65	15.84	0	355	6
RC153	11.416667	144.46	4.87	1416	20
RC158	30.5833333	501.54	6.4	1518	41
RC161	18.8833333	308.22	0	1493	24
RC162	2.9	25.82	6.53	355	14
RC163	27.7	295.92	12.03	3669	6
RC170	4.3	90.12	0	236	32
RC174	1.3	22.53	0	236	8
RC175	4.2666667	80.78	0	329	22
RC176	3.8	90.12	0	236	32
RC191	15.6833333	222.33	11.26	2342	14
RC192	15.5333333	77.75	13.82	3476	6
RC196	6.2	60.2	0	1104	4
RC206	35.6833333	426.28	23.21	3864	6
RC211	18.666667	54.43	37.4	1755	33
RC213	7.4166667	50.22	39.7	875	9

RC214	17.8	50.22	39.7	1755	9
RC215	6.7	53.2	11.84	1399	9
RC216	22.766667	243.67	28.12	3415	42
RC218	11.883333	40.53	23.5	1409	6
RC221	10.816667	32.19	10.99	1760	6
RC223	63.2	198.12	136.76	2271	3
RC224	20.85	206.13	0	449	116
RC225	13.933333	69.05	0	299	29
RC227	6.833333	21.3	10.87	992	36
RC230	9.666667	65.92	14.25	1199	6
RC231	12.133333	41.12	4.35	2599	4
RC232	8.25	51.43	0	607	26
RC236	11.15	22.01	11.62	2739	8
RC243	17.616667	60.34	12.51	3569	3
RC244	23.45	84.53	13.5	4419	6
RC245	31.55	186.72	4.88	2951	35
RC248	46.783333	286.3	12.61	3532	9
RC249	9.166667	23.28	7.08	2025	14
RC257	23.35	98.14	0	4552	4
RC258	20.233333	123.79	5.78	1576	15
RC261	7.516667	10.5	0	2560	2
RC269	34.183333	133.44	4.78	6921	2
RC274	7.033333	4.01	4.18	2562	11
RC284	34.783333	116.54	34.59	6920	2
RC287	44.883333	217.09	12.39	6932	2

Appendix E

Renishaw RenAM 500Q Data

BUILD NAME	TIME (HR)	PART VOLUME (CC)	SUPPORT VOLUME (CC)	NUMBER OF LAYERS	NUMBER OF PARTS
RC289	3.8	42.17	0	783	40
RC290	11.35	33.16	42.68	2606	3
RC291	1.68333333	28.98	0	169	676
RC293	21.2166667	43.77	58.72	2605	4
RC294	1.68333333	28.98	0	169	676
RC296	2.13333333	18.68	0	502	20
RC298	51.05	301.88	4.65	5433	12
RC300	47.7833333	530.44	24.01	6933	12
RC303	12.9333333	569.5	0	2255	27
RC304	49.35	444.21	3.11	7447	9
RC306	11.6166667	62.9	6.34	2102	15
RC307	33.3	173.23	32.35	5854	51
RC309	12.15	80.94	115.56	1224	4
RC310	1.66666667	28.98	0	169	676
RC311	16.5666667	346.78	0	3433	1
RC312	1.66666667	28.98	0	169	676
RC313	8.83333333	85.2	0	2518	2
RC314	18.5	201.85	7.33	2069	130
RC315	8.16666667	42.26	0	1373	32
RC318	8.01666667	105.81	92.12	1522	2
RC320	24.7666667	93.19	53.84	4113	4
RC321	17.7833333	206.62	37.66	5239	2

BIBLIOGRAPHY

- [1] T. Wohlers, "Wohlers Report 2018: Additive Manufacturing and 3D Printing State of the Industry," Wohlers Associates, Inc., 2018. [Online]. Available: <http://wohlersassociates.com/2018report.htm>.
- [2] "Global Additive Manufacturing Market, Forecast to 2025," Frost & Sullivan, 2016.
- [3] ASTM, "Standard Terminology for Additive Manufacturing Technologies," 2012.
- [4] "How Powder Bed Fusion Works," GE Additive, [Online]. Available: <https://www.ge.com/additive/additive-manufacturing/information/powder-bed-fusion>.
- [5] "About Additive Manufacturing: Powder Bed Fusion," Loughborough University, [Online]. Available: <https://www.lboro.ac.uk/research/amrg/about/the7categoriesofadditivemanufacturing/powderbedfusion/>.
- [6] EOS, "Systems and Solutions for Metal Additive Manufacturing," EOS, [Online]. Available: https://www.eos.info/systems_solutions/metal.
- [7] Renishaw, "Metal 3D printing," Renishaw, [Online]. Available: <https://www.renishaw.com/en/metal-3d-printing--32084>.
- [8] SLM Solutions, "SLM Solutions," SLM Solutions, [Online]. Available: <https://www.slm-solutions.com/>.
- [9] 3D Systems, "3D Systems," 3D Systems, [Online]. Available: <https://www.3dsystems.com/>.
- [10] GE Additive, "GE Additive," GE Additive, [Online]. Available: <https://www.ge.com/additive/>.

- [11] S. Dunham, "The Future of Metal 3D Printing Technologies from a New Perspective," SmarTech Publishing, [Online]. Available: <https://www.smartechanalysis.com/blog/category/metal/>. [Accessed 9 April 2020].
- [12] EOS, "EOSTATE Monitoring and Quality Assurance," EOS, [Online]. Available: <https://www.eos.info/software/monitoring-software>. [Accessed 20 March 2020].
- [13] "Why DMP is the DMLS Solution For You.," 3D Systems, [Online]. Available: <https://www.3dsystems.com/dmls-printing-dmp>.
- [14] "EOS EOSINT M 280," Treatstock 3D Printing Services, [Online]. Available: <https://www.treatstock.com/machines/item/220-eosint-m-280>.
- [15] "AM250," Renishaw, [Online]. Available: <https://www.renishaw.com/en/am250--15253>.
- [16] "AM 400," Renishaw, [Online]. Available: <https://www.renishaw.com/en/am-400--35456>.
- [17] "RenAM 500Q," Renishaw, [Online]. Available: <https://www.renishaw.com/en/renam-500q--42781>.
- [18] D. Rosen and S. Yim, "Build Time and Cost Models for Additive Manufacturing Process Selection," *ASME 2012 International Design Engineering Technical Conferences and Computers and Information in Engineering Conference*, vol. 2, pp. 375-382, 2012.
- [19] M. Baumers, M. Holweg and J. Rowley, "The economics of 3D Printing: A total cost perspective," University of Nottingham, 2016.
- [20] H. Piili, A. Happonen, T. Väistö, V. Venkataramanan, J. Partanen and A. Salminen, "Cost Estimation of Laser Additive Manufacturing of Stainless Steel," *Physics Procedia*, vol. 78, pp. 388-396, 2015.

- [21] F. T. Piller, C. Weller and R. Kleer, "Business Models with Additive Manufacturing— Opportunities and Challenges from the Perspective of Economics and Management," *Advances in Production Technology*, pp. 39-48, 2014.
- [22] I. Gibson, D. Rosen and B. Stucker, "Additive Manufacturing Technologies: Rapid Prototyping to Direct Digital Manufacturing," *Springer*, 2010.
- [23] 3DEO, "Additive Manufacturing (3D Printing) for Parts Consolidation," 3DEO, 19 June 2017. [Online]. Available: <https://news.3deo.co/strategy/additive-manufacturing-3d-printing-parts-consolidation>.
- [24] R. E. Laureijs, J. B. Roca, S. P. Narra, C. Montgomery, J. L. Beuth and E. R. H. Fuchs, "Metal Additive Manufacturing: Cost Competitive Beyond Low Volumes," *Journal of Manufacturing Science and Engineering*, vol. 139, no. 8, 2017.
- [25] U.S. Energy Information Administration, "Electric Power Monthly with Data for December 2019," U.S. Department of Energy, Washington DC, 2020.
- [26] EOS, "DMLS - Direct Metal Laser Sintering," [Online]. Available: <https://gpiprototype.com/dmls-direct-metal-laser-sintering>. [Accessed 27 February 2020].
- [27] J. Faludi, M. Baumers, I. Maskery and R. Hague, "Environmental Impacts of Selective Laser Melting," *Journal of Industrial Ecology*, vol. 21, pp. S144-S156, 2017.
- [28] Precision Tooling Service Company, "AM 400," [Online]. Available: <https://ptscmetrology.com/am-400/>. [Accessed 16 February 2020].
- [29] EOS, "Details and Cost," [Online]. Available: <https://engineering.cmu.edu/next/facilities/details-cost.html>. [Accessed 10 November 2019].
- [30] EOS, "Materials for Metal Additive Manufacturing," [Online]. Available: <https://www.eos.info/material-m>. [Accessed 25 March 2019].

- [31] Renishaw, "Inert atmosphere generation," [Online]. Available: <https://www.renishaw.com/en/inert-atmosphere-generation--31885>. [Accessed 6 March 2020].
- [32] J. Weilhammer, "EOSINT M," EOS, April 2011. [Online]. Available: https://webbuilder5.asiannet.com/ftp/2684/EOS__M_280_update%20technology.pdf. [Accessed 2 March 2020].
- [33] Oklahoma State University, "Price Summary for Compressed Gasses and Related Services," [Online]. Available: <https://purchasing.okstate.edu/sites/default/files/documents/oshop/Compressed%20Gas%20Bid%20Price%20Summary.pdf>. [Accessed 30 November 2019].
- [34] M. Barclift, S. Joshi, T. Simpson and C. Dickman, "Cost Modeling and Depreciation for Reused Powder Feedstocks in Powder Bed Fusion Additive Manufacturing," in *Proceedings of the 27th annual international solid freeform fabrication symposium—an additive manufacturing conference*, Austin, 2016.
- [35] PostProcess Technologies, "Yes! Even on 3D Printed Metal!," PostProcess Technologies, 14 November 2017. [Online]. Available: <https://www.postprocess.com/2017/11/automated-post-printing-on-3d-printed-metal/>.
- [36] T. Simpson, "Postprocessing Steps and Costs for Metal 3D Printing," Additive Manufacturing, 21 May 2018. [Online]. Available: <https://www.additivemanufacturing.media/blog/post/postprocessing-steps-and-costs-for-metal-3d-printing>.
- [37] L. Rickenbacher, A. Spierings and K. Wegener, "An integrated cost-model for selective laser melting (SLM)," *Rapid Prototyping Journal*, vol. 19, no. 3, pp. 208-214, 2013.

[38] Netfabb, "What is Netfabb?," Autodesk, [Online]. Available:

<https://www.autodesk.com/products/netfabb/overview>. [Accessed 6 April 2020].

[39] D. S. Thomas and S. W. Gilbert, "Costs and Cost Effectiveness of Additive Manufacturing," *NIST Special Publication*, vol. 1176, 2014.

ACADEMIC VITA OF MATTHEW JOHN MIDEA III

EDUCATION:

Pennsylvania State University, University Park, PA May 2020
Bachelor of Science in Mechanical Engineering
Minor in Economics

Honors in Mechanical Engineering, Schreyer Honors College
Thesis Title: *Build Time and Cost Estimation of Laser Powder Bed Fusion Processes for Metal Additive Manufacturing*
Thesis Supervisor: Dr. Timothy Simpson

Coursework:

Electronic Measuring Systems	Engineering Design
Thermodynamics	Fluid Flow
Finite Element Analysis	Heat Transfer

RELATED EXPERIENCE:

Lutron Electronics, Coopersburg, PA May 2019 - August 2019
Process Engineering Co-op

- Worked in depth on soldering paste deposits during the manufacturing of electronics
- Planned a limits test to determine necessary quality control of product
- Decreased false call rate of the line by increasing limits by 15%
- Explored possible root causes of failures
- Communicated with process owners of several international facilities to solve line failures
- Inspected all the machines for discrepancies in configuration files to make facilities uniform
- Created a new system of reporting the weekly quality of a line to show long term changes

Peter Cremer North America, Cincinnati, OH May 2017 - August 2017
Process Engineering Intern

- Worked independently to solve production floor issues
- Performed a daily and weekly downtime analysis
- Assessed data to find trends and issues within the current process
- Presented technical information to management and floor workers
- Updated Human Machine interface recipes and other centerlines

SKILLS:

Programmed with computer languages such as Python, Matlab, and Java
Worked extensively with the modeling program SolidWorks and CATIA

AWARDS:

Dean's List	Every Semester
Louis A. Harding Memorial Scholarship	August 2019
Tau Beta Pi	January 2018
The President's Freshman Award (Penn State)	April 2017